This is the peer-reviewed, final accepted version for American Mineralogist, published by the Mineralogical Society of America.
The published version is subject to change. Cite as Authors (Year) Title. American Mineralogist, in press.
DOI: https://doi.org/10.2138/am-2021-7917. http://www.minsocam.org/

REVISION 1

SODIUM NANOPARTICLES IN ALKALI HALIDE MINERALS: WHY IS VILLIAUMITE RED AND HALITE BLUE?

Georges Calas [a] ,Laurence Galoisy [a] and Alexis Geisler [a]

[a] *Sorbonne Université, Muséum National d'Histoire Naturelle, CNRS, Institut de Minéralogie, de Physique des Matériaux et de Cosmochimie, IMPMC, 75005 Paris, France*

**corresponding author : Georges Calas, Sorbonne Université, IMPMC, BC 115, 4 place Jussieu 75005 Paris, France. georges.calas@sorbonne-universite.fr*

ABSTRACT

The presence of metal Na nanoparticles causes the bright, thermally unstable colors of villiaumite, NaF, and halite, NaCl. These nanoparticles have been suspected since a long time to be caused by external irradiation. Metal nanoparticles, often referred to as metal colloids, cause surface plasmon resonance effects, characterized by a single Lorentzian-shaped absorption band. The color of these minerals is due to metal Na nanoparticles of 2.5-3 nm. A key point is that the resonance wavelength, which corresponds to the maximum of the absorption band, is inversely related to the value of the refractive index of the embedding mineral. This causes the position of the main absorption band to be offset downwards by 140 nm in halite relative to villiaumite. As a consequence, the optical transmission window is shifted from the long to the short wavelength domain, explaining the color of blue halite and red villiaumite, respectively. Similar refractive

index dependence may explain the purple color of fluorite, caused by metallic Ca nanoparticles. Finally, the origin of the villiaumite irradiation may be the presence of Th-rich (about 8.8wt% ThO_2) nano-inclusions, about 500 nm large, illustrating the specific geochemistry of peralkaline rocks where villiaumite is found.

Keywords: villiaumite, halite, fluorite, peralkaline rocks, color, radiation damage, UV-visible spectroscopy, nanoparticles

INTRODUCTION

One of the outstanding properties of alkali halides is their optical transparency from the vacuum UV to the far infrared. Though they are intrinsically colorless, they sometimes show a thermally unstable coloration, which, in the absence of chemical impurities, has long been recognized to result from radiation damage (e.g., Przibram, 1953; Stormer and Carmichael, 1970). The simplest radiation-induced defect is the so-called F center, i.e. an electron trapped in an anion vacancy. The F center creates a singly occupied electronic level in the band gap, which colors the crystal. The aggregation of two or three F centers on nearest neighbor sites, gives rise to binary M- and ternary R-centers, respectively. Eventually, color centers aggregate to form metallic alkali nanoparticles, also referred to as colloids, caused by an irradiation at room temperature or higher temperatures (see e.g., Schwartz et al., 2008). Optical properties of metal nanoparticles have unique characteristics that give rise to brilliant colors. For instance, during external irradiation of synthetic halite, the change from a yellow color due to *F*-centers to a bright blue color indicates the formation of Na metal nanoparticles (Kreibig and Vollmer, 1995).

Natural halite, NaCl, presents various radiation-induced colors (Zelek et al., 2015), but blue hues with a broad range of saturation are the most frequent (Supplemental Fig. 1). The blue color has been assigned to colloidal Na metal formed by irradiation with ionizing radiation (Rossman, 2010). Radiation defects in halite provide information on the sedimentary history of salt deposits (Sonnenfeld, 1995; Zelek et al., 2014 and 2015) or the stability of nuclear waste repositories (Levy et al., 1983). Recently, they have been used to assess the exposure duration of the surface of icy moons (Poston et al., 2017) and ordinary chondrites (Chan et al., 2018), subject to cosmic radiation. Villiaumite, NaF, is an accessory phase formed during a late pegmatitic stage associated with peralkaline nepheline syenites (Stormer and Carmichael, 1970; Marks and Markl, 2017). It is generally characterized by its intense carmine red color (Supplemental Fig. S2).

The origin of the red color of natural villiaumite has not yet been investigated, though it is suspected to arise from radiation damage (Rossman, 2010). By contrast, blue halite received much attention, with pioneering studies on samples from Strassfurt, Germany (Przibram, 1953; Doyle, 1960; Howard and Kerr, 1960; Arun et al., 2017) and, more recently, Kłodawa, Poland (Wesełucha-Birczynska et al., 2012; Zelek et al., 2014 and 015) and Morleben, Germany (Arun et al., 2017) salt mines. This study shows that the red color of villiaumite is a result of a surface plasmon resonance (Kreibig and Vollmer, 1995) due to Na metal nanoparticles. The optical spectra of blue halite have a similar origin. The outstanding color change between blue halite and red villiaumite is rationalized in terms of the dependence of the wavelength resonance of the nanoparticles on the refractive index of the embedding mineral. The same formalism may be extended to explain the origin of the purple color of fluorite, due to the presence of calcium metallic nanoparticles. The origin of the villiaumite irradiation may be the presence of Th-rich (about 8.8wt% ThO_2) nano-inclusions, about 500 nm large, illustrating the geochemistry of peralkaline rocks where villiaumite is found.

MATERIALS AND METHODS

Villiaumite crystals come from the agpaitic suite of nepheline syenites of the type locality of the Los Archipelago, Guinea (Lacroix, 1908; Moreau et al., 1998). A sedimentary navy blue halite from Strassfurt (Germany) was used for comparison. Optical absorption spectra were measured at room temperature and at 10K in the spectral range 200–3300 nm (50,000 cm^{-1}- 3,030 cm^{-1}), using a double-beam computerized Perkin-Elmer Lambda 1050 UV–Visible-NIR spectrophotometer. The spectral resolution varies from 0.8 nm in the UV region to 2 nm in the near IR - visible region. A He-cryostat under vacuum (around 3.4×10^{-7} mbar) was used to record spectra at 10 K. The optical absorption spectra were obtained in transmission mode on cleaved crystals (Supplemental Fig. S3). The spectra were normalized to sample thickness and background corrected using a polynomial function. The data are presented and analyzed as a function of wavelength, as the absorption is caused by surface plasmon resonance effects interpreted in terms of the Mie theory (see e.g., Kreibig and Vollmer, 1995). Preliminary scanning electron microscopy with field emission gun (SEM-FEG) analyses were obtained at 15 kV and a beam current of 200 nA with a Zeiss Ultra 55 instrument fitted with a high-resolution Schottky FEG and a UHR Gemini® column. Semi-quantitative analyses were performed using a Bruker Quantax XFlash 4010 energy-dispersive X-ray spectrometer.

RESULTS AND DISCUSSION

Optical absorption spectra of villiaumite

The samples investigated present an intense red color, which disappears in a couple of minutes at 500 °C and after 2 hrs at 400°C. The room temperature optical absorption spectrum (Supplemental Fig. S4) shows the presence of a background due to light scattering by inclusions

and fractures that result from the easy {100} cleavage of this cubic mineral. After subtracting this background contribution, the most salient feature is an intense absorption band at 494 nm, which extends over most of the visible spectrum because of its tail extending at long wavelengths. The two other contributions are a shoulder near 415 nm and a small band at 328 nm (Fig. 1). This spectrum is similar to the one of villiaumite from Mont Saint Hilaire, Canada (Rossman, 2010), which is dominated by a main absorption band peaking at 510 nm.

The optical absorption spectra have been fitted using a minimum of components, chosen to correspond to spectroscopic events. Gaussian and Lorentzian lineshapes of the spectral components have been tested. Indeed, by contrast to the Gaussian shape of absorption bands caused by color centers (see e.g. Jenkins et al., 2000; Hoya et al., 2017), surface plasmon resonances exhibited by metallic nanoparticles give rise to Lorentzian-shaped absorption bands, as predicted by Mie theory (Kreibig and Vollmer, 1995; Seinen et al., 1994; Ruiz-Fuertes et al., 2019). A good fit of the main band is achieved by using a Lorentzian function peaking at 494 nm. The full width at half-maximum (FWHM) of this band, 86 nm, is larger than that of the other contributions due to color centers. This lineshape explains the presence of a long tail extending towards long wavelengths, at the origin of the intense red hue of villiaumite. Such a Lorentzian line-shape characterizes the optical spectra of free neutral Na clusters (Selby et al., 1991), Na nanoparticles in NaCl (Seinen et al., 1994) and NaF (Seifert et al., 1994) or Ca nanoparticles in CaF_2 (Ruiz- Fuertes et al., 2019; Ryskin et al., 2020).

The two minor contributions at 328 nm and 414 nm have a Gaussian lineshape. The former corresponds to a *F*-center, widely investigated in synthetic NaF (Seifert et al., 1994; Tiwald et al., 2015; Hoya et al., 2017). The latter may be assigned to a *R*-center (Amenu-Kpodo and Neubert, 1965; Bryukvina and Martynovich, 2012; Bryukvina et al., 2018). Recent ab-initio calculations

(Tiwald et al., 2015; Hoya et al., 2017) have shown that the absorption energy E_a of the *F*-center (in eV) may be approximated by:

$$E_a = 16.5\ a^{-1.76} \quad (1)$$

where a is the anion-cation distance. Relation (1) gives a physical ground to the classical empirical Mollwo-Ivey relation (Ivey, 1947). The predicted values, 345 ands 415 nm, are in good agreement with the experimental values, 328 and 414 nm. In the optical absorption spectrum of villiaumite from Mont Saint Hilaire, Canada (Rossman, 2010), the main absorption band at 510 nm shows a slightly different lineshape and additional weak contributions around 400 nm. As in natural blue halite (Zelek et al., 2015), the relative proportion of isolated defect centers and metallic nanoparticles may vary among the samples.

Evidence of a plasmon resonance in villiaumite

As indicated above, a Lorentzian lineshape is consistent with a surface plasmon resonance. The position of this resonance is similar to that in synthetic NaF (Chandra and Holcomb, 1969; Bryukvina and Martynovich, 2012; Bryukvina et al., 2018). The resonance wavelength may be predicted from the Mie theory by considering spherical metal particles (Doyle, 1958; Hunault et al., 2017). In this approximation, the average size of the nanoparticles is derived from:

$$R = V_f \lambda_p^2 / (2\pi c \Delta\lambda) \quad (2)$$

where R is the average radius of the metallic clusters, V_f is the Fermi velocity of the electrons in the bulk metal (for Na, $V_f = 1.07 \times 10^6$ m.s^{-1}), λ_p is the characteristic wavelength at which the surface plasmon resonance (SPR) occurs, $\Delta\lambda$ is the full width at half-maximum and c is the speed of light. This predicts an average diameter of Na nanoparticles slightly smaller than 3 nm. At 10 K, this absorption band only slightly shifts by about 10 nm towards higher wavenumbers, without any narrowing. This is consistent with an assignment to a surface plasmon resonance, which does

not change in energy or amplitude with temperature, by contrast to the transitions related to color centers (Kreibig and Vollmer, 1995).

Color centers in alkali halides have a limited thermal stability above room temperature relative to Na colloids, (Schwartz et al., 2008). This explains why, in the geological samples, a plasmon resonance is predominant over the electronic transitions expected from these color centers. Similar mechanisms have been observed in glasses where alkali ions can act as electron traps upon irradiation and form metal colloids (Boizot et al., 2000). Such processes are thermally activated and demonstrate that alkali ions agglomerate to form bigger complexes after trapping electrons at temperatures reaching a few hundreds °C.

Comparison with halite

The shape of the optical absorption spectrum of blue halite from Stassfurt is similar to some of the blue halites above mentioned. It is almost identical to the first absorption spectra published on blue halite (also from Stassfurt: Doyle, 1960) (Supplemental Fig. S5). The main absorption band peaks at 640 nm, the same value as reported by previous authors (e.g., Doyle, 1960; Howard and Kerr, 1960). Using several Gaussian-Lorentzian spectral components, assigned to Na colloids and various color centers, gives a good fit (Zelek et al., 2014 and 2015). However, fitting the spectra is non equivocal. Here, we use a minimum number of spectral components, as for villiaumite. The main band, at 640 nm, is fitted with a single Lorentzian component (Fig. 2), because it arises from a surface plasmon resonance of Na nanoparticles (e.g., Seinen et al., 1994). The FWHM, 105 nm, is similar to the values found in the Klodawa mine (Wesełucha-Birczyńska et al., 2012) and larger than in villiaumite (86 nm) . Minor additional Gaussian-shape contributions at 430, 531 and 744 nm may be assigned to *F*-, *R*- (3 neighboring *F*-centers) and *M* (2 neighboring *F*-centers) color centers, respectively. The actual position of these bands is shifted relative to that

166 expected from relation (1), at 473, 550 and 705 nm for the *F*-, *R*- and *M*-centers-, respectively.
167 The same centers are found in the halite from Klodawa mine and a similar discrepancy with the
168 Mollwo-Ivey relation is observed (Wesełucha-Birczyńska et al., 2012). Finally, a fourth minor
169 Gaussian contribution occurs at 385 nm as in other natural halites (Doyle, 1960; Wesełucha-
170 Birczyńska et al., 2012), but its origin is unclear.
171
172 **Scaling the spectra of red villiaumite and blue halite**
173 The halite spectrum presents similarities with that of villiaumite, but occurs at larger
174 wavelengths. As a consequence, the transmission window does not occur in the same spectral
175 region, being located on the long or short wavelength side of the main band in red villiaumite and
176 blue halite, respectively (Figs. 1 and 2). This explains the difference in the color of these minerals,
177 despite both show a broad Lorentzian shape plasmon resonance with spectral properties
178 independent of temperature, which is assigned to the presence of Na nanoparticles. For spherical
179 particles that are smaller than the wavelength of light, the value of the resonance wavelength
180 depends on the refractive index of the surroundings (Kreibig and Vollmer, 1995). The
181 wavelength of maximum absorption λ_{max} may be predicted within the Mie theory, following the
182 Doyle relation (Doyle, 1958; Davenas et al., 1973; Seifert et al., 1994):
183 $$\lambda_{max}=\lambda_c(1+2n_0^2)^{1/2} \quad (3)$$
184 where n_0 is the refractive index of the host medium and λ_c is the critical wavelength for the onset
185 of ultra-violet transparency of sodium. The ratio between the λ_{max} values in villiaumite and halite,
186 allows elimination of the λ_c term. The ratio calculated from the refractive index of these minerals
187 is 1.13 to compare to an experimental value of 1.29. This explains qualitatively the redshift of the
188 plasmon band with the increasing refractive index of the mineral. The underestimation of this

shift when using relation (3) may come from non-spherical shape effects or size distribution of the Na colloids in geological samples with a complex history relative to laboratory samples…

IMPLICATIONS

The comparison of the optical absorption spectra of halite and villiaumite provides a nice illustration of Mie theory, through the dramatic influence of the refractive index of halides on the energy of the plasmon resonance of the embedded metal nanoparticles. Temperatures up to 300-500°C (Zelek et al., 2015; Weerkamp et al., 1994), crystal dislocations and substituted impurities favor the aggregation of color centers leading to the formation of Na colloids. This explains the predominance of these colloids in natural halides (Seifert et al., 1994), as demonstrated by their bright colors. The formation of Na colloids goes with that of free dihalogen molecules, as in the villiaumite from Kola Peninsula, Russia (Celinski et al., 2016) and can only occur once the crystal cooled down to avoid the annealing of these colloids. It is of interest that natural purple fluorites also owe their color to the presence of Ca nanoparticles. Their optical absorption spectra show an intense, broad absorption band near 560 nm that has been suggested to come from Ca metal colloids (Bill and Calas, 1983; Rossman, 2010; Gaft et al., 2020; Ryskin et al., 2020). The same band is found in additively colored synthetic CaF_2 (Angervaks et al., 2018). This absorption band has a Lorentzian shape, which indicates a plasmon resonance origin (Ryskin et al., 2020). Its position, near 560 nm, is intermediate between that in red villiaumite, 494 nm, and blue halite, 640 nm. This absorption band allows light transmission in both the red and blue regions of the spectrum, resulting in the characteristic purple color of irradiated fluorites. It may be pointed out that the position of the colloid band ranges in the order villiaumite (494 nm)-fluorite (560 nm)-halite (640 nm), i.e. the same ranking as for the refractive indices, 1.3253, 1.4338 and 1.5442, hence qualitatively following the prediction of Relation (3).

Natural halite exhibits a broad range of colors, navy-blue, blue, purple or colorless arising from various proportions of color centers and Na colloids (Wesełucha-Birczynska et al., 2012). Zelek et al. (2014) have shown that this may result from the complex sedimentary geology that governs in the mine the spatial distribution of halite and sylvinite, as ^{40}K is suspected to be the main radiation source. In villiaumite, radiation damage is caused by a specific geological context. Agpaitic rocks are always enriched in Th and U (Sorensen, 1992). Though XRD only indicates the presence of NaF, preliminary SEM-EDS investigations of our samples (Fig. 3) show the presence of nanospheres, about 500 nm large, which show a preferential alignment that apparently guides the {100} cleavage steps. These nanoinclusions contain about 8.8wt% ThO_2 (Supplemental Fig. S6) and may be at the origin of a permanent irradiation of the mineral, able to create defects once the mineral cooled down to a few hundreds °C. This explains the presence of isolated color centers, which otherwise have a limited thermal stability (Schwartz et al., 1994) and the stability of the Na nanoparticles that are at the origin of the red color. The presence of thorium in the villiaumite from the Khibiny and Lovozero alkaline massifs in the Kola Peninsula, Russia (Chukanov et al., 2006) has been explained by its complexation by organic matter, which was revealed by infrared spectroscopy. Preliminary infrared spectra on the villiaumite from the Los Archipelago also reveal the presence of aliphatic hydrocarbon groups and carboxylates in our samples (A. Geisler, unpublished report). The red color of villiaumite, prized in mineral collections, appears to be also a useful "color indicator" of the conditions of emplacement of the evolved stages of peralkaline systems.

ACKNOWLEDGMENTS

We are grateful to Jean-Claude Boulliard for providing the samples and their pictures from the mineral collection of Sorbonne-Université, Maxime Guillaumet for his help on the IMPMC

spectroscopy platform and Imene Esteve for the preliminary SEM analyses. We thank Charles Geiger and George Rossman for fruitful suggestions that greatly improved the manuscript.

REFERENCES CITED

Amenu-Kpodo, K., and Neubert, T.J. (1965) Color centers in sodium fluoride. Journal of Physics and Chemistry of Solids, 26,1615-1619.

Angervaks, A.E., Veniaminov, A.V., Stolyarchuk, M.V., Vasilev, V.E., Kudryavtseva, I., Fedorov, P.P., Ryskin, A.I. (2018) Optical study of calcium precipitates in additively colored CaF_2 crystals. Journal of the Optical Society of America B, 35, 1288-1294.

Arun, T., Ram, S. S., Karthikeyan, B., Ranjith, P., Ray, D. K., Rout, B., Krishna, J. B. M., Sengupta, P., and Satyam, P.V. (2017) Ion beam radiation effects on natural halite crystals. Nuclear Instruments and Methods B, 409, 216-220.

Bill, H., and Calas G. (1978) Color centers, associated rare-earth ions and the origin of coloration in natural fluorites. Physics and Chemistry of Minerals, 3, 117-131.

Boizot, B., Petite, G., Ghaleb, D. Pellerin, N., Fayon, F., Reynard, B., and Calas, G. (2000) Migration and segregation of sodium under β-irradiation in nuclear glasses. Nuclear Instruments and Methods B, 166, 500–504.

Bryukvina, L., Ivanov, N., and Nebogin, S. (2018) Relationships between lithium and sodium nanoparticles and color centers formation in LiF and NaF crystals with hydroxide and magnesium ions impurities. Journal of Physics and Chemistry of Solids, 120,133-139.

Bryukvina, L.I., and Martynovich, E.F. (2012) Formation and properties of metallic nanoparticles in lithium and sodium fluorides with radiation-induced color centers. Physics of the Solid State, 54, 2374-2378.

Celinski, V.R., Ditter, M., Kraus F., Fujara F., and Schmedt auf der Günne, J. (2016) Trace determination and pressure estimation of fluorine F_2 caused by irradiation damage in minerals and synthetic fluorides. Chemistry-A European Journal, 22,18388–18393.

Chan Q. H. S., Zolensky M. E., Kebukawa Y., Fries M., Ito M., Steele A., Rahman Z., Nakato A., Kilcoyne A. L. D., Suga H., Takahashi Y., Takeichi Y., and Mase K. (2018) Organic matter in extraterrestrial water-bearing salt crystals. Science Advances 4, eaao3521.

Chandra, A., and Holcomb, D.F. (1969) Taxonomy of F-aggregate centers in NaF. Journal of Chemical Physics, 51, 1509–1523.

Chukanov, N.V., Pekov, I.V., Sokolov, S.V., Nekrasov, A.N., Ermolaeva, V.N., and Naumova, I.S. (2006) On the problem of the formation and geochemical role of bituminous matter in pegmatites of the Khibiny and Lovozero alkaline massifs, Kola Peninsula, Russia. Geochemistry International, 44, 715-728.

Davenas, J., Perez, A., Thevenard, P., and Dupuy, C.H.S. (1973) Correlation between absorption bands and implanted alkali ions in LiF. Physica Status Solidi A, 19, 679–686

Davidson, A.T., Kozakiewicz, A.G., Comins, J.D., and Derry, T.E. (1996) Optical effects in NaF crystals implanted with 100 keV ions. Nuclear Instruments and Methods B, 116, 216-219.

Doyle, W.T. (1958) Absorption of light by colloids in alkali halide crystals. Physical Review, 111, 1067-1072.

Doyle, W.T. (1960) Coagulation, optical absorption and photoconductivity of colloid centres in alkali halides. Proceedings of the Physical Society, 75, 649–663.

Gaft, M., Waychunas, G.A., Rossman, G.R., Nagli, L., Panczer, G., Cheskis, D., and Raichlin, Y. (2020) Red photoluminescence and purple color of naturally irradiated fluorite. Physics and Chemistry of Minerals, 47**,** 46.

Howard, C.L.H., and Kerr, P.F. (1960) Blue halite. Science, 132,1886-1887.

Hoya, J., Laborde, J.I., Richard, D., and Renteria, M. (2017) Ab initio study of F-centers in alkali halides. Computational Materials Science, 139, 1-7.

Hunault, M., Loisel, C., Bauchau, F., Lemasson, Q., Pacheco, C., Pichon, C., Moignard, B., Boulanger, K., Hérold, M., Calas, G., and Pallot-Frossardt, I. (2017) Nondestructive redox quantification reveals glassmaking of rare French gothic stained glasses. Analytical Chemistry, 89, 6277-6284.

Ivey, H.F. (1947) Spectral location of the absorption due to color centers in alkali halide crystals. Physical Review, 72, 341–343.

Kikuchi, A. and Ozawa K. (1973) Induced F aggregate centres in NaF crystals irradiated with charged particles at low temperature. Physica Status Solidi A, 18, 567-578.

Kreibig, U., and Vollmer, M. (1995) Optical properties of metal clusters. Springer: Berlin/Heidelberg.

Lacroix, A. (1908) Sur l'existence du fluorure de sodium cristallisé comme élément des syénites néphéliniques des îles de Los. Comptes Rendus Hebdomadaires des Séances de l'Académie des Sciences, 146, 213-216.

Levy, P. W., Loman, J. M., Swyler, K. J., and Klaffty, R. W. (1983) Radiation damage studies on synthetic NaCl crystals and natural rock salt for radioactive waste disposal applications. In: Scientific Basis for Nuclear Waste Management, Ed. P.L. Hofman, 136–167.

Marks, M.A.W., and Markl, G. (2017) A global review on agpaitic rocks. Earth-Science Reviews, 173, 229–258.

Moreau, C., Ohnenstetter, D., Demaiffe, D., and Robineau, B. (1998) The Los Archipelago nepheline syenite ring-structure: a magmatic marker of the evolution of the Central and Equatorial Atlantic. Canadian Mineralogist, 34, 281–299.

Okada, T. (2006) Nano-scale particles of mixed alkali-metals in KCl crystals. Journal of the Physical Society of Japan, 75, 094705.

Poston, M.J., Carlson, R.W., and Hand, K.P. (2017) Spectral behavior of irradiated sodium chloride crystals under Europa-like conditions. Journal of Geophysical Resarch, Planets, 122, 2644–2654.

Przibram K. (1953) Verfärbung und Lumineszenz. Beiträge zur Mineralphysik. Springer-Verlag, Vienna.

Rossman G.R. (2010) Mineral spectroscopy server. Caltech. https ://doi.org/10.7907/JYWR-QQ57.

Ruiz-Fuertes, J., Ibáñez, J., Monteseguro, V., Alencar, I., and Cazorla, C. (2019). Reversible tuning of Ca nanoparticles embedded in a superionic CaF_2 matrix. The Journal of Physical Chemistry C, 123, 19945–19951.

Ryskin, A.I., Fedorov, P.P., Lushchik, A., Generalov, M.E., Angervaks, A.E., Stolyarchuk, M.V., Vasil'chenko, E., and Kudryavtseva, I. (2020) Absorption spectrum of dark purple fluorite, Kent deposit, Kazakhstan. Journal of Fluorine Chemistry**,** 240, 109654.

Schwartz, K., Volkov, A.E., Sorokin, M.V., Trautmann, V.C., Voss, K.O., Neumann, R., and Lang, M. (2008) Effect of electronic energy loss and irradiation temperature on color-center creation in LiF and NaCl crystals irradiated with swift heavy ions. Physical Review B, 78, 024120.

Seifert, N., Ye, H., Tolk, N., Husinsky, W., and Betz G. (1994) The influence of defects and defect clusters on alkali atom desorption stimulated by low energy electron bombardment of alkali halides. Nuclear Instruments and Methods B, 84, 77-88.

Selby K., Kresin, V., Masui, J., Vollmer, M., de Heer, W.A., Scheidemann, A., and Knight, W.D. (1991) Photoabsorption spectra of sodium clusters. Physical Review B, 43,4565-4572.

Sonnenfeld, P. (1995) The color of rock salt -a review. Sedimentary Geology, 94, 267-276.

Sørensen, H. (1992) Agpaitic nepheline syenites—a potential source of rare elements. Applied Geochemistry, 7, 417-427.

Stormer, J.C., and Carmichael, I. (1970) Villiaumite and the occurrence of fluoride minerals in igneous rocks. American Mineralogist, 55, 126-134.

Tiwald, P., Karsai, F., Laskowski, R., Gräfe, S., Blaha, P., Burgdörfer, J., and Wirtz, L. (2015) Ab initio perspective on the Mollwo-Ivey relation for F centers in alkali halides. Physical Review B, 92, 144107.

Weerkamp, J.R. W., Groote, J.C., Seinen, J., and Den Hartog, H.W. (1994) Radiation damage in NaCl. I. Optical-absorption experiments on heavily irradiated samples. Physical Review B, 50, 9781– 9786.

Wesełucha-Birczynska, A., Zelek, S., and Stadnicka, K. (2012) Blue halite colour centre aggregates studied by micro-Raman spectroscopy and X-ray diffraction. Vibrational Spectroscopy, 60 124–128.

Zelek, S.M., Stadnicka, K.M., Tobola,T., and Nowak, L.N. (2014) Lattice deformation of blue halite from Zechstein evaporate basin: Klodawa Salt Mine, Central Poland. Mineralogy and Petrology, 108, 619-631.

Zelek, S.M., Wesełucha-Birczyńska, A., Szklarzewicz, J., and Stadnicka, K.M. (2015) Spectroscopic properties of halite from Klodawa salt mine, Central Poland. Mineralogy and Petrology, 109, 45–51.

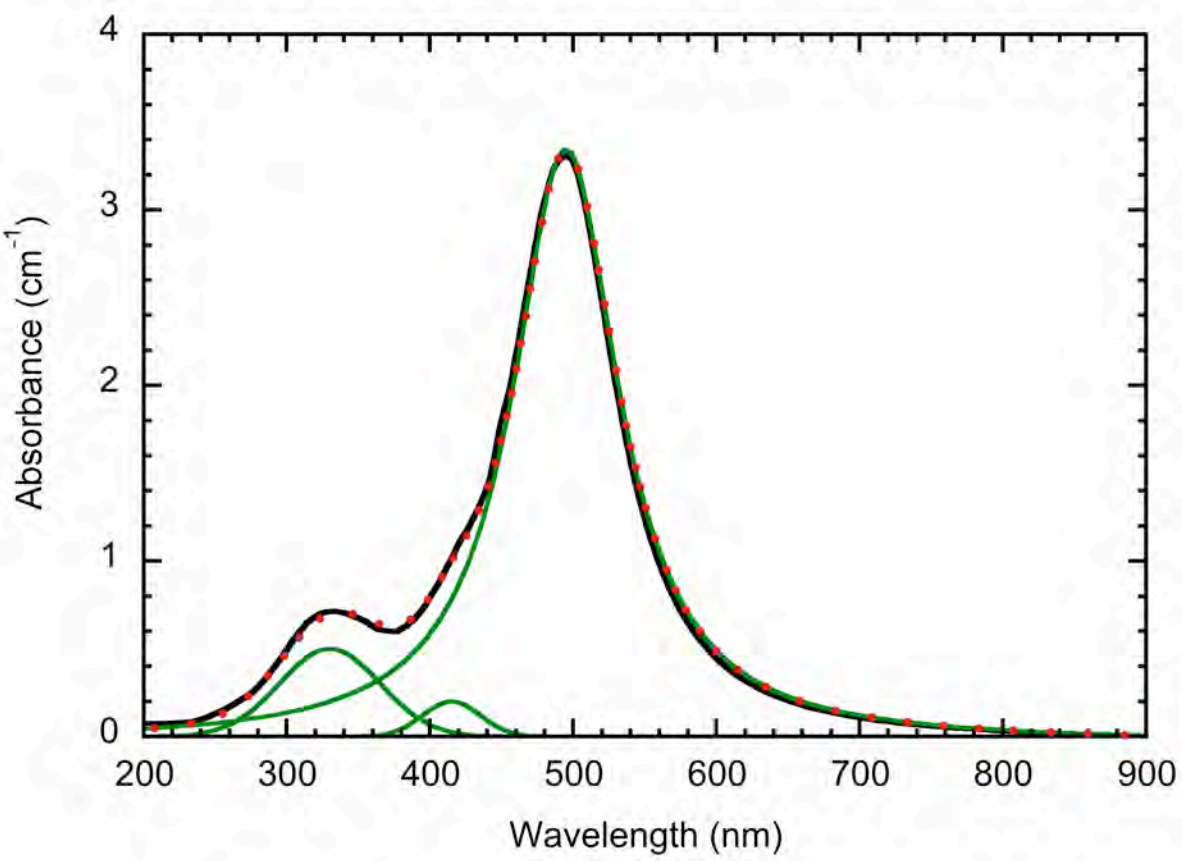

Figure 1. Room temperature optical absorption spectrum of red villiaumite from nepheline syenites of the Los Archipelago, Guinea. The optical spectrum has been background corrected for light scattering caused by crystal inhomogeneities. The main band, assigned to surface plasmon resonance for metallic Na, shifts by about 140 nm in halite relative to villiaumite. As a consequence, light is transmitted in the long wavelength side of the main absorption band. The fit uses a Lorentzian function for the surface plasmon resonance (main band) and Gaussian components for the minority color centers. The functions used for the fit are displayed in green. The resulting fit gives the red dots.

This is the peer-reviewed, final accepted version for American Mineralogist, published by the Mineralogical Society of America.
The published version is subject to change. Cite as Authors (Year) Title. American Mineralogist, in press.
DOI: https://doi.org/10.2138/am-2021-7917. http://www.minsocam.org/

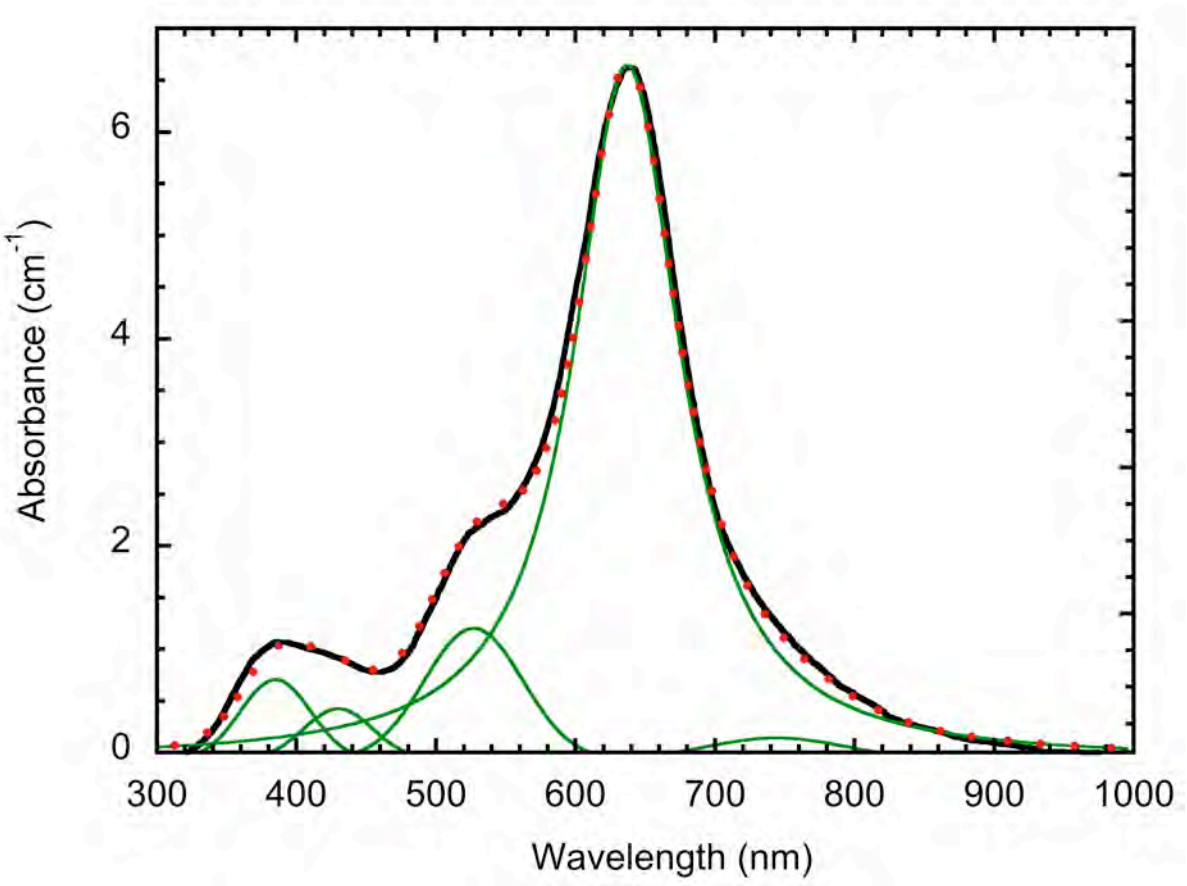

Figure 2. Room temperature optical absorption spectrum of blue halite from Stassfurt, Germany, background corrected for light scattering by crystal inhomogeneities. The main band shifts by about 140 nm relative to villiaumite. As a consequence, light is transmitted in the short wavelength side of the main absorption band, hence the spectacular color difference. The fit uses a Lorentzian function for the surface plasmon resonance (main band) and Gaussian components for the minority transient color centers. The functions used for the fit are displayed in green. The resulting fit gives the red dots.

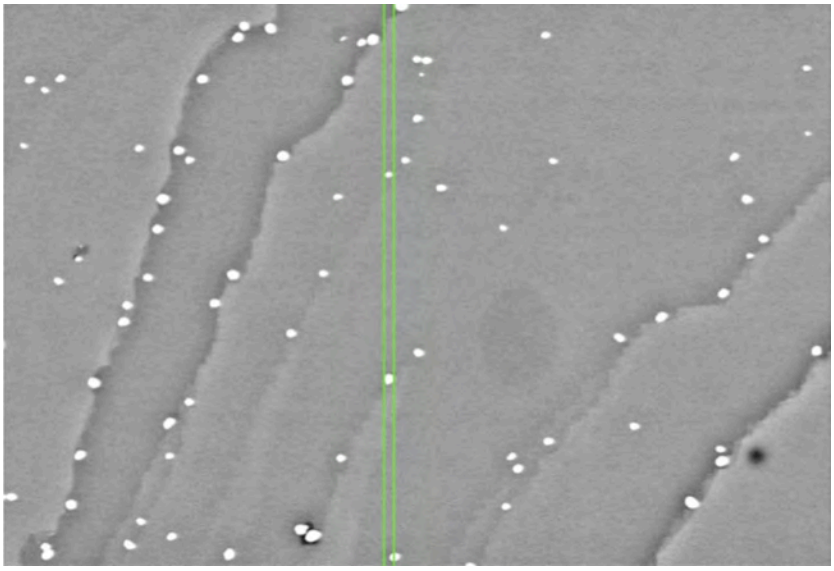

Figure 3. Scanning Electron Microscopy micrograph in backscattered electron mode of a villiaumite cleavage, showing the presence op thorium-rich nano-inclusions. The scale is given by the green bars, separated by 500 nm. EDS analysis of these nano-inclusions (Supplemental information, Fig. S6) shows that thorium is only accompanied by minor amounts of uranium. The apparent alignment of these inclusions inherits from the growth of the mineral, in which they guide the {100} cleavage steps. These solid inclusions are thought to cause a permanent internal irradiation of the mineral. Once the villiaumite-bearing rock cools down to low temperatures, typically below 400°C, this irradiation will progressively cause the formation of radiation-induced color centers and metallic Na nanoparticles at the origin of the intense red coloration, characteristic of villiaumite.

This is the peer-reviewed, final accepted version for American Mineralogist, published by the Mineralogical Society of America.
The published version is subject to change. Cite as Authors (Year) Title. American Mineralogist, in press.
DOI: https://doi.org/10.2138/am-2021-7917. http://www.minsocam.org/

REVISION 1

Supplemental Material

Figure S1. Blue halite (Sample # N00341_AJM4313) from Stassfurt, Germany (Mineral Collection, Sorbonne Université, Paris).

Figure S2. Red villiaumite (Sample # N13100_AJM5773) from the Los Islands Archipelago, Guinea (Mineral Collection, Sorbonne Université, Paris).

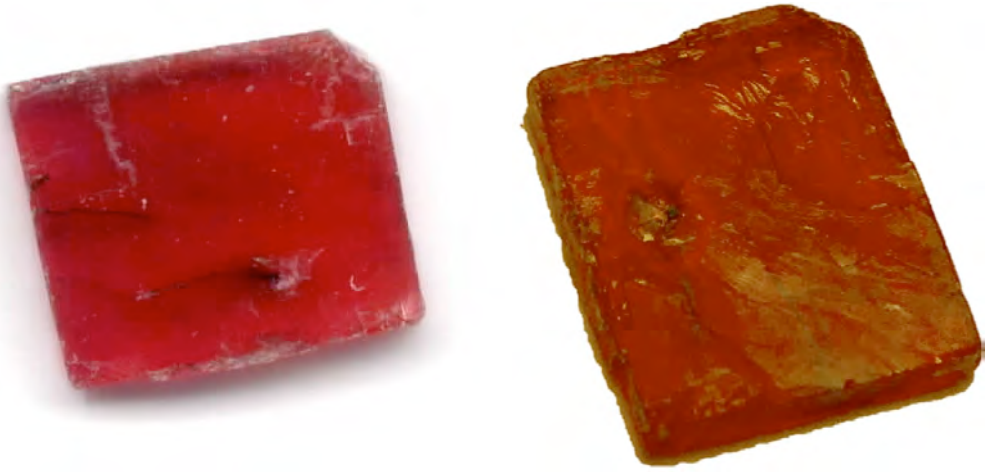

Figure S3. Cleavage section of euhedral crystals of villiaumite from the Los Islands Archipelago, Guinea.

This is the peer-reviewed, final accepted version for American Mineralogist, published by the Mineralogical Society of America.
The published version is subject to change. Cite as Authors (Year) Title. American Mineralogist, in press.
DOI: https://doi.org/10.2138/am-2021-7917. http://www.minsocam.org/

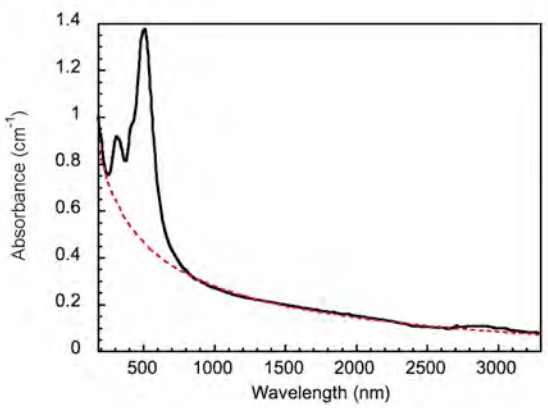

Figure S4. Room temperature optical absorption spectrum of villiaumite. The dotted red line corresponds to the background absorption due to a scattering of the incident light by optical heterogeneities (inclusions and fractures)

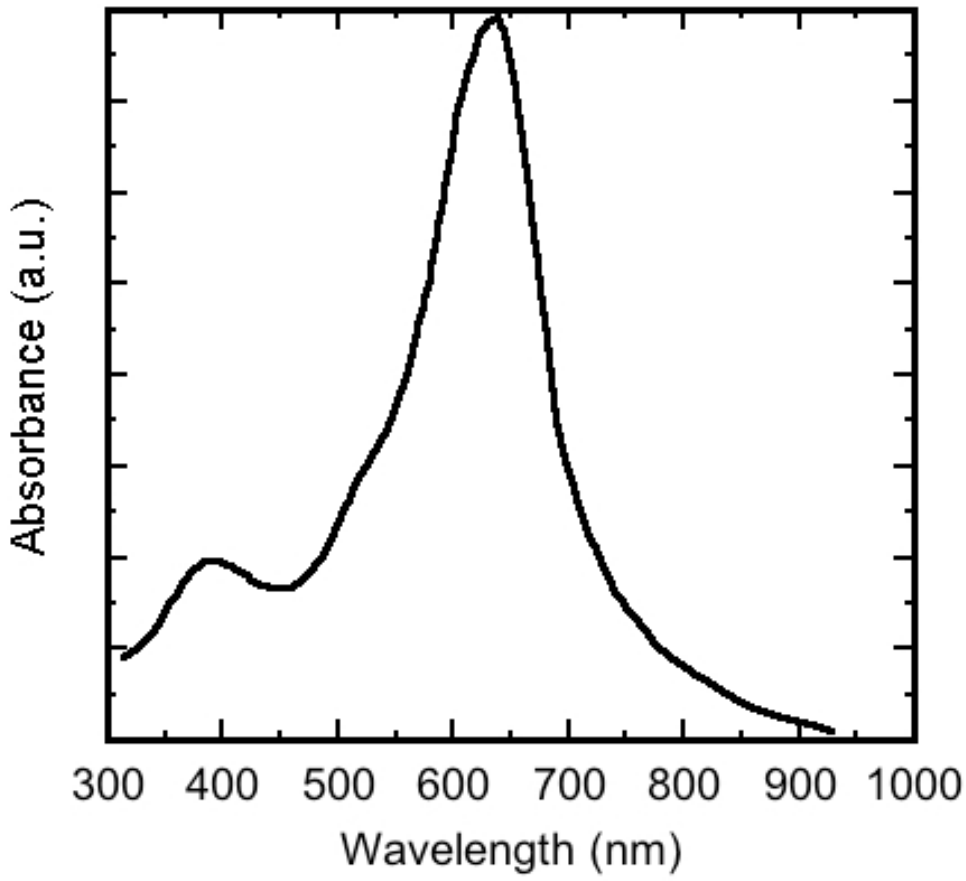

Figure S5. Scan of the historical absorption spectrum of the natural blue Stassfurt halite published by Doyle in 1960. The main absorption band peaks at 640 nm, a value consistent with that reported in this study.

This is the peer-reviewed, final accepted version for American Mineralogist, published by the Mineralogical Society of America.
The published version is subject to change. Cite as Authors (Year) Title. American Mineralogist, in press.
DOI: https://doi.org/10.2138/am-2021-7917. http://www.minsocam.org/

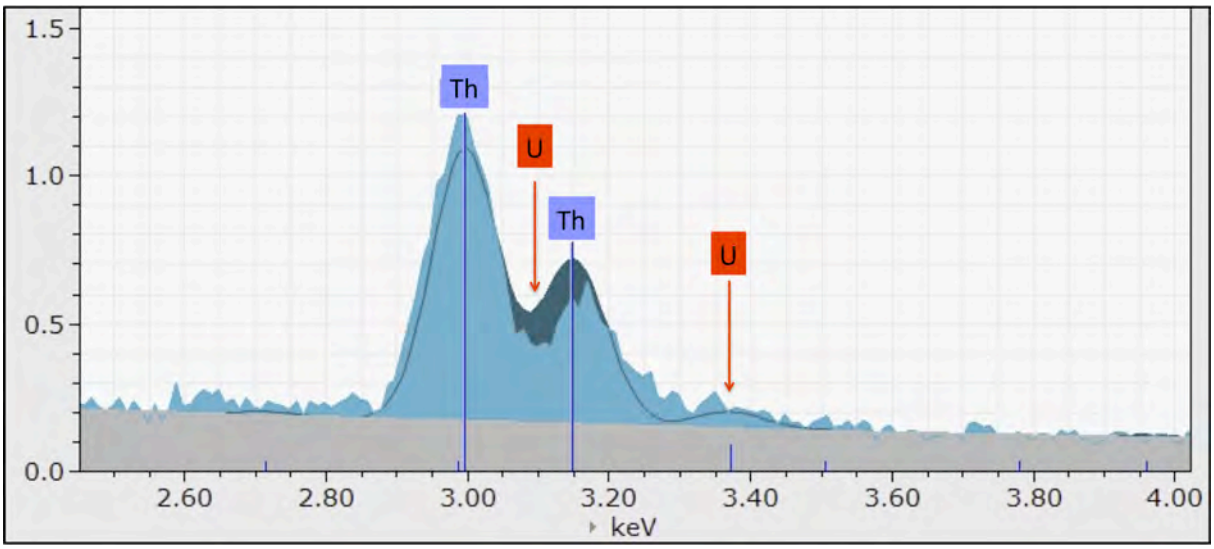

Figure S6. SEM/energy-dispersive X-ray spectroscopy of the nanoinclusions ,about 500 nm large, encountered in the villiaumite from the Los Archipelago and depicted in Figure 2. The Th concentration has been calculated using the fit of the Th-Mα_1 and Th-Mβ_1 signals, at 2.996 and 3.149 keV, respectively. The weak contribution at 3.35-3.40 keV may arise from the U-Mβ_1 signal, expected at 3.336 (the signal expected for U-Mα_1 at 3.171 keV is hidden by the more intense Th-Mβ_1 emission).

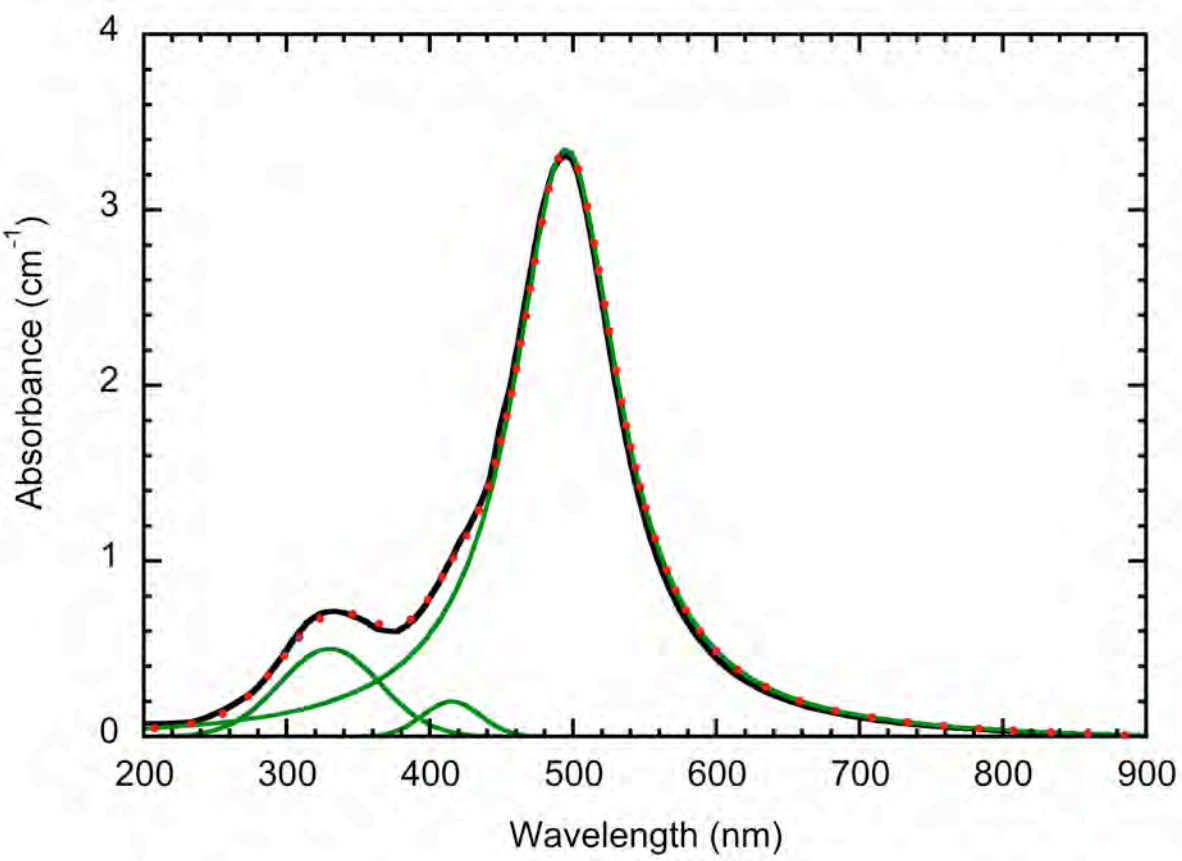

Figure 1. Room temperature optical absorption spectrum of red villiaumite from nepheline syenites of the Los Archipelago, Guinea. The optical spectrum has been background corrected for light scattering caused by crystal inhomogeneities. The main band, assigned to surface plasmon resonance for metallic Na, shifts by about 140 nm in halite relative to villiaumite. As a consequence, light is transmitted in the long wavelength side of the main absorption band. The fit uses a Lorentzian function for the surface plasmon resonance (main band) and Gaussian components for the minority color centers. The functions used for the fit are displayed in green. The resulting fit gives the red dots.

This is the peer-reviewed, final accepted version for American Mineralogist, published by the Mineralogical Society of America.
The published version is subject to change. Cite as Authors (Year) Title. American Mineralogist, in press.
DOI: https://doi.org/10.2138/am-2021-7917. http://www.minsocam.org/

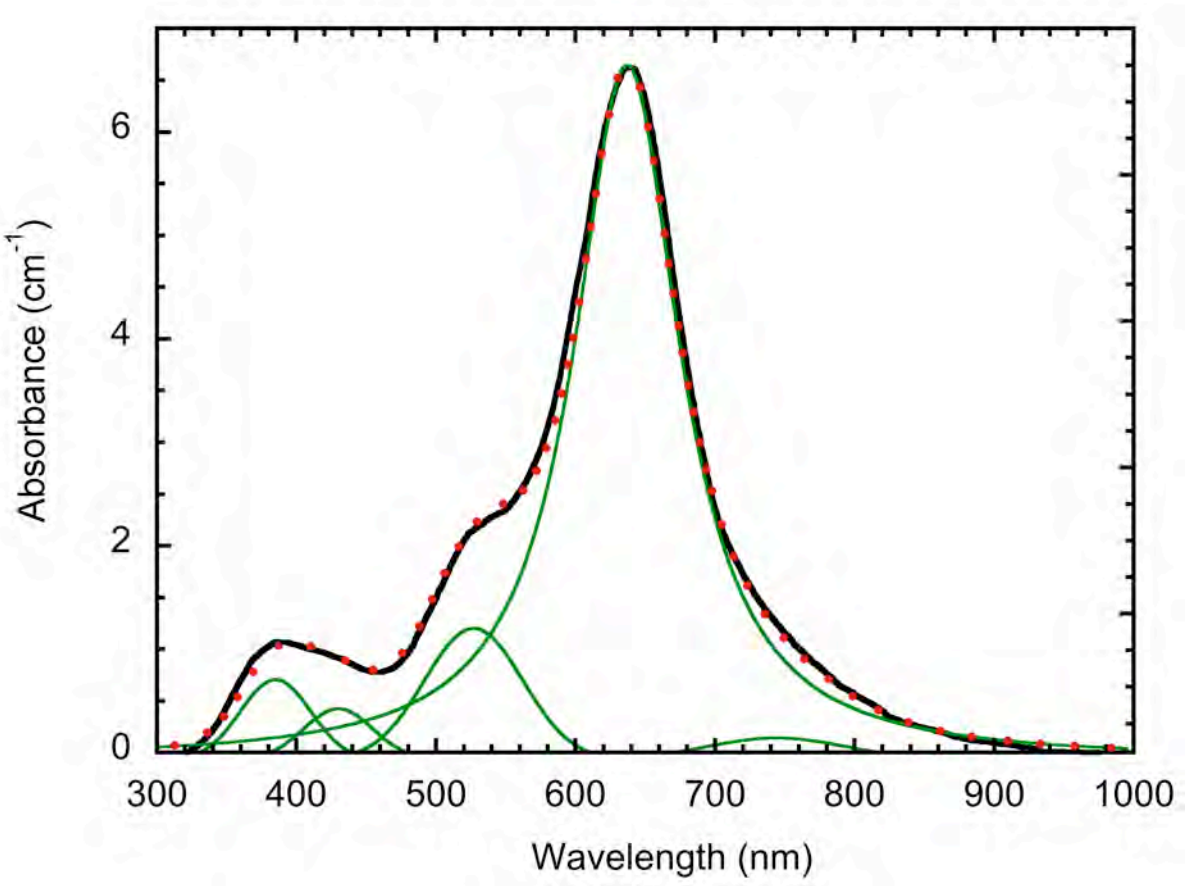

Figure 2. Room temperature optical absorption spectrum of blue halite from Stassfurt, Germany, background corrected for light scattering by crystal inhomogeneities. The main band shifts by about 140 nm relative to villiaumite. As a consequence, light is transmitted in the short wavelength side of the main absorption band, hence the spectacular color difference. The fit uses a Lorentzian function for the surface plasmon resonance (main band) and Gaussian components for the minority transient color centers. The functions used for the fit are displayed in green. The resulting fit gives the red dots.

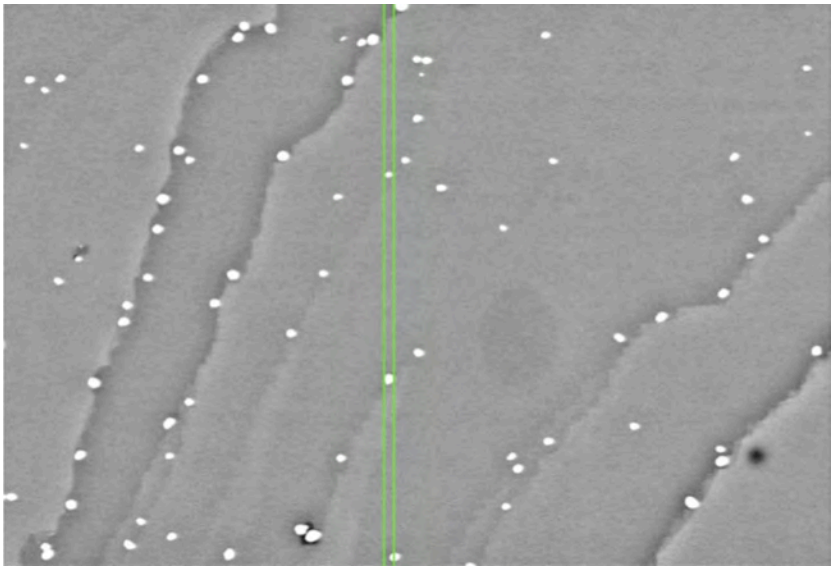

Figure 3. Scanning Electron Microscopy micrograph in backscattered electron mode of a villiaumite cleavage, showing the presence op thorium-rich nano-inclusions. The scale is given by the green bars, separated by 500 nm. EDS analysis of these nano-inclusions (Supplemental information, Fig. S6) shows that thorium is only accompanied by minor amounts of uranium. The apparent alignment of these inclusions inherits from the growth of the mineral, in which they guide the {100} cleavage steps. These solid inclusions are thought to cause a permanent internal irradiation of the mineral. Once the villiaumite-bearing rock cools down to low temperatures, typically below 400°C, this irradiation will progressively cause the formation of radiation-induced color centers and metallic Na nanoparticles at the origin of the intense red coloration, characteristic of villiaumite.